

Structure, Mechanical Properties and Oxidation Resistance of Iso and Non-Iso Architected TiN/Cr Multilayers Coatings Deposited by Magnetron Sputtering

Vagner F. G. Soares^{a*} , Daniel A. Ramirez^a , Igor Z. Damasceno^b, Fernando G. Echevirrigaray^c ,
Carlos A. Figueroa^d, Bruna L. Perotti^d, Francisco L. Serafini^d, Givanilson B. Oliveira^a ,
André R. Terto^a , Eduardo K. Tentardini^a 

^aUniversidade Federal de Sergipe, Av. Marechal Rondon, S/N, São Cristóvão, SE, Brasil

^bUniversidade Federal do Rio Grande do Norte, Av. Senador Salgado Filho, 3000, Natal, RN, Brasil

^cUniversidade Estadual de Campinas (UNICAMP), Instituto de Física “Gleb Wataghin”, 13083-970, Campinas, SP, Brasil

^dUniversidade de Caxias do Sul, Rua Francisco Getúlio Vargas, 1130, Caxias do Sul, RS, Brasil

Received: July 15, 2020; Revised: October 27, 2020; Accepted: November 27, 2020

Iso and non-iso architected TiN/Cr multilayers with constant composition were deposited by balanced magnetron sputtering aiming to investigate the influence of different architectures over coatings structures and properties. Glow discharge optical emission spectroscopy analyses were used to determine in-depth constituents and suggested that no diffusion of elements occurred between layers in room temperature. Field emission gun scanning electron microscopy analyses showed that all multilayers presented sharp interfaces and low porosity microstructures, with column-like grain growth influenced by layer sizes. Glancing angle X-ray diffraction analyses showed that multilayers consist of polycrystalline α -Cr and δ -TiN phases with a main peak in Cr(110) plane. The overlapping of TiN onto metallic layers led to the suppression of growth in the TiN(111) plane, although TiN layers thicker than 50 nm demonstrated a growth in plane TiN(200). Nanoindentation tests registered equal hardness values for all multilayers of around 16.2 GPa, on the other hand, a tendency to improve hardness has been identified for hierarchical multilayer. Oxidation tests revealed that architectures with thicker TiN top layers presented an improved oxidation resistance up to 600 °C, probably due to growth in more compact TiN(200) plane. However, TiN/Cr coatings did not resist integrally to oxidation tests at 750 °C.

Keywords: Coatings, magnetron sputtering, TiN/Cr multilayers, non-iso architectures, high temperature oxidation.

1. Introduction

Thin films with high hardness are commonly applied to cutting tools, gears and bearings, aiming to protect against premature failure and enhance lifespan when facing ever-increasing thermomechanical demands. Despite the existence of individual layer coatings, those assembled with multilayers of different materials periodically distributed along the thickness tend to present improved wear, corrosion and oxidation resistances¹⁻³. Such enhanced properties are mainly attributed to the presence of discontinuities among different layers, which significantly suppress cracks propagation and diffusion of chemical compounds along the internal structure. Furthermore, multilayer thin films can reduce the excess of residual stress and restrict the columnar growth, which is common to ceramic coatings, thus favoring a stronger adhesion to substrates^{4,5}.

In general, the combination of two distinct layers in a thin film is called bilayer or period. Traditionally, multilayers are formed in an isostructural configuration with constant

period, and the main variables considered when structuring such films are: period size, thickness layers ratio in a period, number of periods and total coating thickness⁶.

Even so, service failures remain a relevant topic to isostructured multilayers⁷⁻⁹. On account of commonly being structured with repeated bilayers, vulnerabilities encountered in a certain period tend to be replicated to the others since deterioration mechanisms are analogously materialized along thickness.

In contrast, it has been demonstrated that alternating periods with different configurations in a film can provide dynamic responses to externally applied demands. In this context, non-iso architectures such as *hierarchical multilayers*, in which the period size gradually decreases from the base to the surface, and *graded multilayers*, in which composition gradients are inserted along thickness, have been reported to show greater tenacity when compared to isostructured multilayers¹⁰.

Some other advantages can be acquired by mixing different periods in non-isostructured coatings: since different layer sizes

*e-mail: eng.vagsoares@gmail.com

may induce the formation of phases with distinct crystalline structures^{2,11-13}, materials properties can be varied along the coating thus resulting in more advanced elasto-plastic or diffusional effects. Advantageously, once the variation in films architecture by magnetron sputtering (MS) can be obtained only by redistributing layer sizes, no physical adjustment is necessary to produce such coatings. As a physical deposition method, controlling the deposition time of each layer is enough to effectively modify the periods sizes.

In the last years, several combinations of materials have been used in the structuring of multilayers^{1-4,7-8,14}, among which chromium (Cr) and titanium nitride (TiN) have shown expressive results. Nam et al.¹⁴ deposited a TiN/Cr bilayer by magnetron sputtering on 316L steel and recorded a decrease in substrate corrosion current density from 115.650 $\mu\text{A}/\text{cm}^2$ to 1.201 $\mu\text{A}/\text{cm}^2$, with 98.96% protection efficiency for a bilayer TiN/Cr ~ 300 nm/700 nm. In another study, Ezazi et al.¹⁵ structured TiCr/TiCrN multilayers and recorded a reduction in friction coefficient of the AL7075-T6 substrate from 0.3 to approximately 0.1. Also, XIAO group¹⁶ has studied TiN/Cr bilayers evaluating the resistance to thermal shocks at 800 °C, 1000 °C and 1200 °C.

Despite showing significant results, however, the influence of different architectures on structure and properties of TiN/Cr multilayers coatings remain a potential and undeveloped topic in literature up to date.

The present work aims to investigate the influence of varying architectures on structure, mechanical properties and oxidation resistance of TiN/Cr multilayer coatings. All coatings were deposited by MS with a systematically varied distribution of layers along each sample in order to assemble an isostructured and three types of non-isostructured multilayers. Composition was purposefully kept constant for all multilayers in order to attribute any property change solely to architectures variation. Energy-Dispersive X-ray Spectroscopy (EDS), Field-Emission Gun scanning electron microscopy (SEM-FEG), Glow-discharge optical emission spectroscopy (GD-OES) and Glancing angle X-ray diffraction (GAXRD) were used to investigate structures and architectures as well as nanoindentation and oxidation tests to assess the resulting properties.

2. Materials and Methods

Coatings were deposited in a balanced magnetron sputtering configuration, using AJA Orion 5-HV equipment with Cr (99.99%) and TiN (99.85%) targets, both with 2.0" diameter placed in DC (7.5 W/cm²) and RF (31.3 W/cm²) power supplies, respectively. The base pressure was 10⁻⁵ Pa, the work pressure was set in 4 \times 10⁻¹ Pa of argon and estimated deposition rates in previous conditions were 3.7 nm/min and 3.0 nm/min for Cr and TiN, respectively. Once the aim of this work is to evaluate the influence of architecture on TiN/Cr multilayers, no bias nor external heating was applied for coating deposition, in order to limit the number of variables influencing the films. A schematic diagram of deposition process is presented in Figure 1.

Silicon wafers and polished AISI 304 stainless steel plates were adopted as substrates. Substrate surfaces were cleaned in ultrasonic baths before each deposition. Four different types of multilayers were deposited, as shown in Figure 2.

Individual layers were achieved by the opening/closing of shutters in pre-determined times. Multilayers were built with 800 nm total thickness, divided in layers of 50 nm for TM sample and 20, 40, 60 and 80 nm for non-iso-architected samples M1, M2 and M3.

Traditional multilayer (TM) was chosen to represent the isostructured architecture commonly found in literature^{1,9,17}. The other three comprise of non-iso architectures in which: M1 sample presents an hierarchical architecture, developed in recent years for mechanical properties optimization^{10,18}, whereas M2 and M3 samples were designed with different metal/nitride ratios in each period, aiming to distribute Cr and TiN gradients along thin film cross sections and form designs close to the graded architecture concept¹⁹⁻²¹. In M2, TiN quantity raises from bottom to top while in M3 a raise of Cr occurs in this same direction (see Figure 2).

All multilayers were designed as to contain equal Cr and TiN amounts. Therefore, the existing variations on structure and properties among them can only be evaluated as a function of the singular architecture.

Coatings elemental characterization was carried out by EDS with JEOL JCM 5700 equipment. Carl Zeiss Auriga scanning electron microscope with field emission gun (SEM-FEG) equipment was used for cross-section analyses.

In-depth composition profiles were evaluated by GD-OES in Horiba GD-Profil2 equipment, applying pressure of 400 Pa, RF-power source of 30 W and 0.01 data points acquired per second. Crystalline structures of all films were characterized

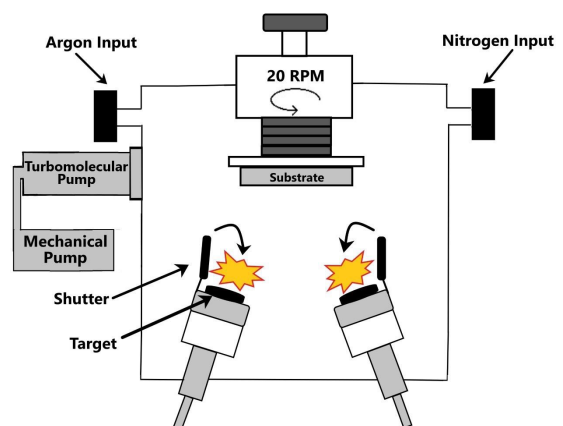


Figure 1. Schematic representation of deposition chamber.

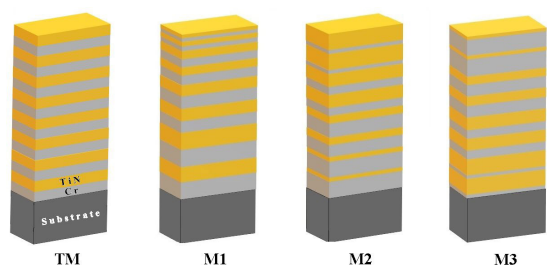


Figure 2. Schematic representation of multilayers architectures.

by GAXRD with Shimadzu XRD-6000 equipment, Cu-K α radiation ($\lambda = 1,54 \text{ \AA}$) and incident angle of 5° .

Nanoindentation tests were executed in MicroMaterials NanoTest-600 nanodurometer, coupled with Berkovich indenter. Load/unload rate was 0.1 mN/s, with a normal initial load of 0.1 mN and load maximum permanence time of 5 s. Maximum penetration depth was defined in 10% of the films thickness. Results were calculated from 20 indentations and penetration followed Oliver-Pharr method²².

Oxidation tests of coatings deposited onto silicon wafers with 1 cm^2 were carried out in muffle oven at 400°C , 600°C and 750°C with no vacuum application. Heat rate was maintained constant at $10^\circ\text{C}/\text{min}$ and the permanence time at maximum temperature for each test was set in 4 hours. After the heating cycle, films were cooled to ambient temperature inside the oven. The purpose of these experiments was to evaluate structure degradation and the resistance of different architectures against high temperature oxidation.

3. Results

3.1 Composition, architecture and morphology

EDS analyses indicated that TiN/Cr multilayers are composed by similar Cr/Ti ratios, near to 1.2, revealing a regular composition of approximately 54.5 at.% Cr and 45.5 at.% TiN for all deposited coatings. Constant composition among films enables for performance differences to be related to architectural variation only. The elemental in-depth

constitution will be discussed further on GD-OES analyses. Multilayers exhibited a hard layer amount close to half of the composition, which have already been reported as suitable for balancing high hardness with low residual stresses⁹.

Cross section micrographs were initially registered for multilayers architecture analyses, as shown in Figure 3a-d. All samples present clear and dark lines related to Cr and TiN layers, respectively, revealing that the ceramic and metallic materials alternate along thickness. Each film possesses eight layers of Cr and eight layers of TiN. Measurements performed in micrographs disclose total films thicknesses of 800 nm.

Upon comparison, it is possible to note that, with exception of iso-structured TM sample, there is a variation in individual layers thicknesses inside the films. TM is comprised by 50 nm layers, with a constant period size of 100 nm (Figure 3a). This same period size was maintained in samples M2 and M3, however, these films possess layers varying in 20, 40, 60 and 80 nm aiming to provide periods with composition gradients along the thickness.

In M2 graded multilayer (Figure 3c), the thinnest TiN layers are located at the base of the film and their thicknesses gradually grow to the surface whereas an opposite distribution is observed in M3 graded coating (Figure 3d). On the other hand, M1 sample presents layers ordered according to a size hierarchy: both 80 nm layers of Cr and TiN at the base periods and 20 nm layers at the top (Figure 3b). The cross-sectional images also reveal the formation of microstructures with a low pore density as well as defined and sharp interfaces for all multilayers.

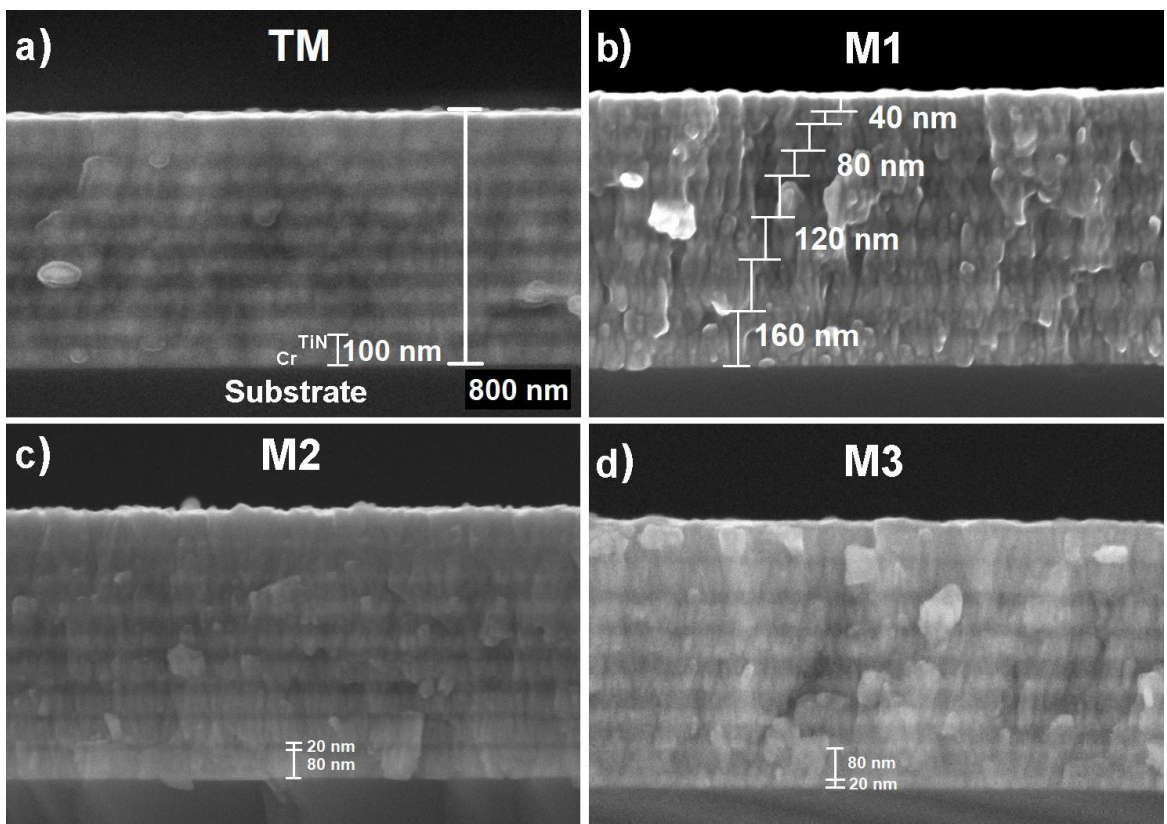


Figure 3. Micrographs of multilayers cross-sections (a) TM, (b) M1, (c) M2 and (d) M3 with magnification of 50000x.

From cross section of M1 hierarchical multilayer (Figure 3b) it is also possible to observe that the structure is formed by grains of varied aspects. While the 20 nm layers present small grains with a few indistinguishable boundaries for both materials, the 80 nm layers present prominent column-like grains and the center region, formed mainly by 60 nm layers, show intermediate sized grains, evidencing a direct relation between layer thicknesses and grain growth. Periods with 120 and 160 nm presented columnar grains whereas smaller periods revealed microstructures in which this grain shape was restricted by layer size.

Multilayers M2 and M3 presented similar behavior to sample M1: columns were evidenced in layers thicker than 60 nm, although thinner layers (<50 nm) demonstrated a suppression of columnar growth. Such observation is in line with the findings of Cr layers by Li et al.²³, where Cr interlayers with 45 nm did not evidence the columnar structure. On the other hand, TM sample with 50 nm layers presented a dense microstructure with prominence of scattered columnar grains, thus suggesting this layer size as transitional for the appearance of column-like grains in deposited TiN/Cr systems.

GD-OES technique was employed in order to better analyze in-depth composition. The results are explicit in Figure 4 with each identified layer (L) signaled. Magnifications of TiN regions are shown in inserts and the elements iron (Fe) and chromium from steel substrate are also identified.

In Figure 4, the first identified signal occurs for TiN layers, which decrease subsequently as Cr starts to be registered. It is also observed that Cr peaks occurred in Ti valley regions, and vice-versa. Nitrogen identification followed a similar behavior as Ti as well, evidencing that N atoms are also restricted to TiN layers. Additionally, all graphs present varying peak widths for each element, corresponding to the films varying layers sizes in the multilayers systems.

In this sense, sample M1 has increasing peak widths as a function of the analysis depth, with the first peaks of each element related to 20 nm layers and the last to 80 nm layers. In this context, it is evidenced that iso architected TM and hierarchical M1 films surfaces are comprised by periods with TiN/Cr ratios of 1/1 while graded multilayers M2 and M3 surfaces consist of periods with TiN/Cr ratios equal to 1/4 and 4/1, respectively. Hence, there is a singular architecture and in-depth elemental distribution for each film, although they all have the same total composition.

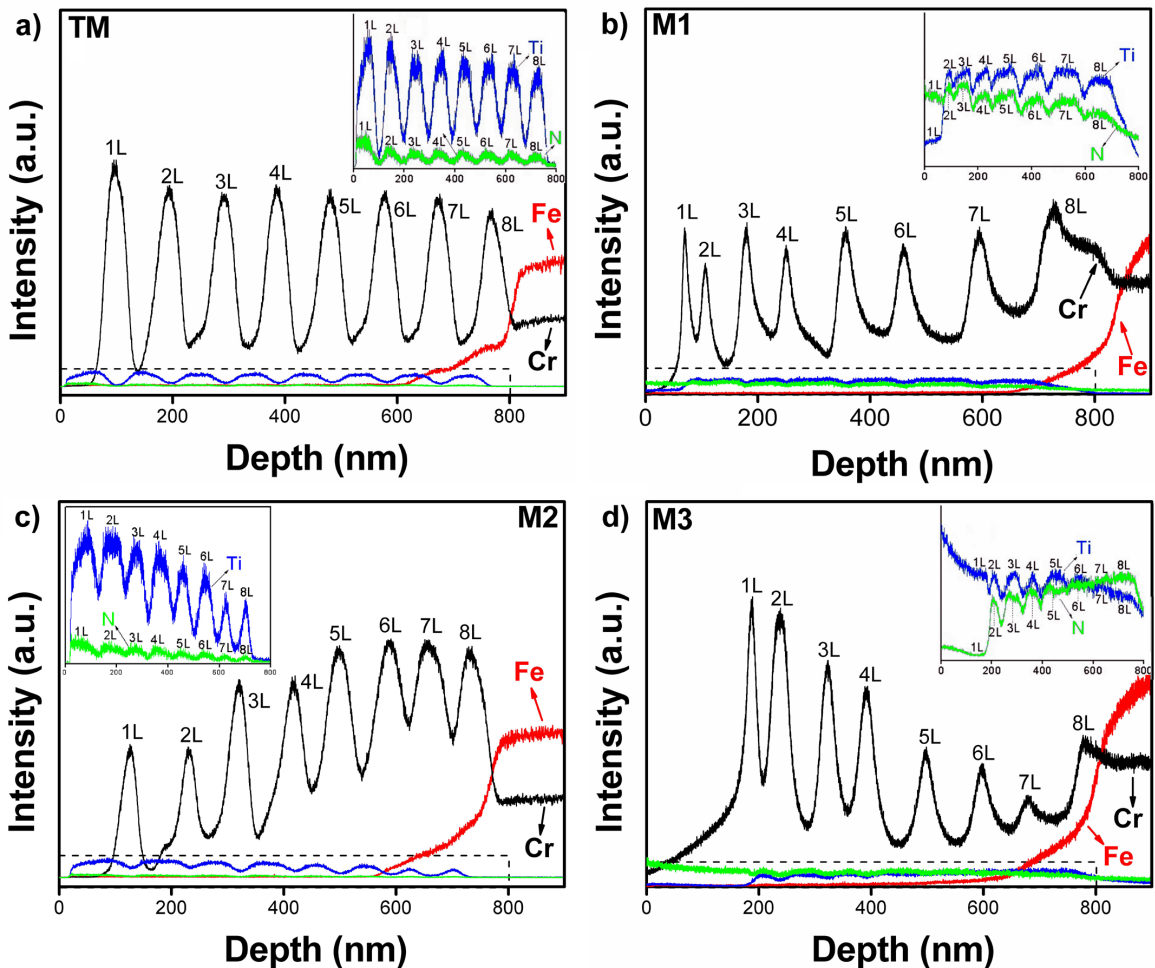


Figure 4. GD-OES profiles of TiN/Cr multilayers (a) TM, (b) M1, (c) M2 and (d) M3. Ti and N signals are evidenced in insets.

3.2 Crystalline structure

Coatings were subjected to GAXRD to evaluate existing crystalline structures. The patterns obtained for all films are explicit in Figure 5a. Pure chromium manifested a main peak in plane (110) located at $2\theta = 44.1^\circ$ and additional growth in planes (200) and (211) located at positions 64.2° and 81.8° , respectively, indicating the body-centered cubic α -Cr phase. In parallel, pure TiN film presented a main peak in plane (111) at 36.4° and planes (200), (220) and (311) at 42.2° , 61.4° and 73.7° positions, respectively, indicating the formation of face-centered cubic δ -TiN phase. Given the different positions of TiN(111) and Cr(110) peaks, it is assumed that the $\text{TiN}_{\text{FC}}/\text{Cr}_{\text{CC}}$ phases originally have a high mismatch lattice degree.

Multilayers analyses revealed a main peak in Cr(110) plane with diffuse signals for TiN phase peaks, and an intense reduction of TiN(111) peak previously recorded as preferential in the pure TiN coating. Such effect is probably attributed to distortions generated at interfaces and the subsequent reorganization of nitride atoms in order to overcome the high mismatch lattice degree between Cr and TiN original structures²⁴.

GAXRD analyses indicate that multilayers are composed by polycrystalline structures, but the overlap of TiN to the metallic layers probably lead to the amorphization of its structure. Even so, the peaks recorded for both phases indicate the maintenance of a high mismatch degree at the interfaces, suggesting them as incoherent, what corroborates with the sharp interfaces seen in microscopy analyses (Figure 3a-d).

However, TiN(200) diffraction peak presented a slight better definition in M2 sample pattern, what is likely attributed to the thicker TiN layers of 80 nm on the surface. In order to confirm such assumption, GAXRD analyses with incident angle of 1° were also acquired for all multilayers, as seen in Figure 5b. For TM and M2 samples with thicker TiN top layers, the peak TiN(200) increased and Cr(110) relatively decreased. On the other hand, for M1 and M3 films in which TiN top layers are thinner (~ 20 nm), the peaks still showed a sparse signal. Therefore, it is assumed that crystallinity of the layers probably increases with the thickness, once TiN

top layers with 20 nm present less defined TiN(200) peaks than 50 and 80 nm top layers.

Although TiN/Cr interfaces are not effective to determine how columnar growth affects the crystallinity level, given that TiN(200) plane emerged only for multilayers TM and M2, with top layers thicker than 20 nm, it can be suggested that the TiN columnar-like growth of thicker layers is parallel to an increase crystallinity effect. The plane TiN(200), recorded to the thicker layers, possesses an interplanar distance more similar to Cr(110) plane than to TiN(111) ($d_{\text{TiN}(111)} = 2.4636$ nm, $d_{\text{TiN}(200)} = 2.1315$ nm e $d_{\text{Cr}(110)} = 2.0581$ nm). This growth tendency of TiN/Cr multilayers in plane TiN(200) was also observed by Nam et al.¹⁴ and confirms that TiN growth is influenced by Cr layers.

In this context, since constituent layers along thickness vary only in distribution order, the crystalline structure of layers with same thickness are not expected to be distinct and the relative signal variations in TiN peaks acquired with incidence angle of 5° are attributed to the different architectures among films. Therefore, it is evidenced that TiN top layers of the films have contributed differently to acquired signals.

GAXRD analyses did not show signs of TiCrN phase formation, nor common peak shift phenomenon attributed to the formation of this ternary nitride by solid solution²⁵⁻²⁷. Furthermore, as plane TiN(200) is naturally more compact than TiN(111), the growth trend in TiN(200) plane revealed by GAXRD corroborates with the low porosity structures observed in cross section micrographs.

3.3 Mechanical properties

Figure 6 presents nanohardness tests results for deposited TiN/Cr multilayers. All measurements were carried out with a constant penetration depth of 80 nm (10% of films thickness). Measured hardness value for pure TiN and Cr films were 18.6 GPa and 8.5 GPa, respectively, and for TM iso architected multilayer the registered value was 16.3 GPa. Such hardness is below the one registered for pure TiN, though it surpasses the one calculated by rule of mixtures for these materials. The hardness values closer to that of TiN occurs, primarily, due to sixteen internal interfaces.

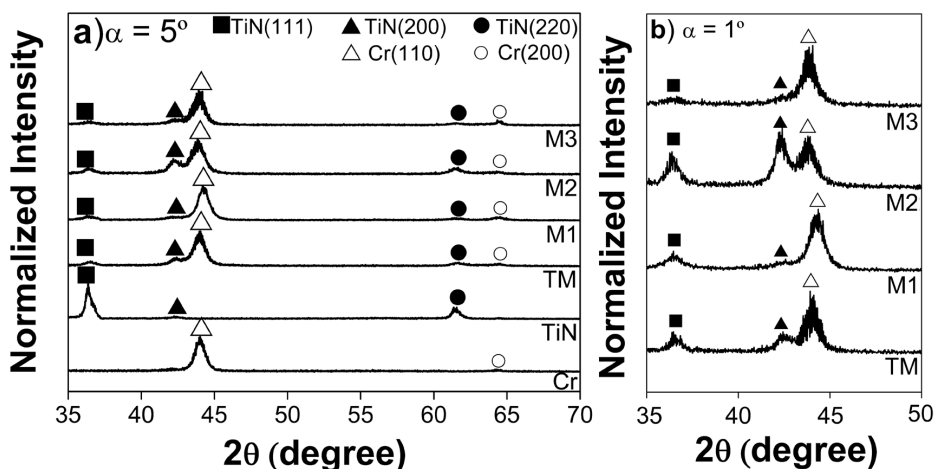


Figure 5. GAXRD patterns of as deposited coatings acquired with incidence angle of (a) 5° and (b) 1° .

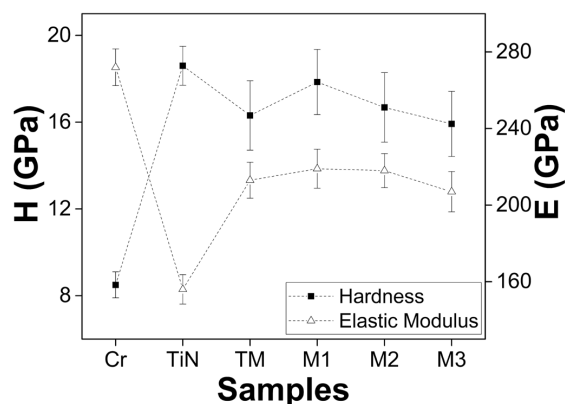


Figure 6. Hardness and elastic modulus of as deposited TiN/Cr coatings.

The other multilayers presented statistically similar values, as can be seen in Table 1. Given that hardness is a measurement of localized plastic deformation, the similar values indicate that multilayers possessing both equal compositions and number of interfaces, even with distinct architectures, do not tend to present relevant variation in hardness values. Therefore, the produced multilayers tend to develop similar behaviors when subjected to localized external loads that tension the entire interior of the coatings. These observations may suggest that in other metal/nitride systems similar effects can be found, being the variation of the number of internal interfaces and the construction of different layer sizes important variables to be monitored for hardness optimization.

Young's modulus values for all samples obtained through nanoindentation resulting curves are also shown in Table 1. Young's modulus of chromium and titanium nitride were registered as 272 and 156 GPa, respectively, and for isostructured TM multilayer the recorded value was 213 GPa. Thus, differently than observed for hardness, Young's modulus tended to follow the rule of mixtures. Such fact reveals that the interfaces did not significantly influence this property and the composition is the main governing variable for Young's modulus. The other multilayers presented statistically similar E values, as can be seen in Figure 5.

H/E and H^3/E^2 values, used to predict the elastic strain to failure and resistance against plastic deformation, respectively, were also calculated. Values are shown in Table 1. H/E multilayer ratios were about 0.08, which is higher than that found for the Cr/CrN system¹, which has a hardness value like those found for multilayers produced in the present work. However, H/E values below 0.1 suggest that TiN/Cr multilayers tend to present nanoplastic deformation, being not capable of well distributing loads along thickness when external forces are applied²⁸.

In parallel, H^3/E^2 values were similar for all multilayers and exceeded the previously mentioned Cr/CrN system and others such as TiAlSiN/CrN¹³ and TiSiN/Ni¹⁷. Nevertheless, all values around 0.95 are somewhat below those considered optimal for coatings with high wear resistance^{28,29}. From that, it is noted the high hardness values of TiN/Cr multilayers jointly with maintenance of considerable Young's modulus

Table 1. H, E, H/E and H^3/E^2 values of as deposited thin films.

Sample	H (GPa)	E (GPa)	H/E	$H^3/E^2 \times 10^{-1}$
Cr	8.5 ± 0.6	272 ± 9.6	0.02	0.03
TiN	18.6 ± 0.9	156 ± 7.7	0.12	2.40
TM	16.3 ± 1.6	213 ± 9.4	0.08	0.95
M1	17.9 ± 1.5	219 ± 10.2	0.08	0.98
M2	16.7 ± 1.6	218 ± 8.9	0.08	0.97
M3	15.9 ± 1.5	207 ± 10.5	0.08	0.94

values reveals that the combination of such materials in multilayers results in sensitive structures to high and moderate impact mechanical demands, being adequate only for low intensity contact applications.

M1 sample with hierarchical architecture did show a tendency to improve deformation resistance, suggesting that its distribution order of layers may improve tribological performance, as evidenced by Rivera-Tello group^{10,30}. Such effect is related to its highest hardness value of 17.9 GPa, an increment that must be attributed to decreasing the period size towards the surface. This kind of architecture promotes a boundary strengthening in the top half of the film due to the higher density of interfaces preventing dislocation movement, as suggested by Hall-Petch relation^{31,32}.

3.4 Oxidation resistance

Pure Cr and TiN coatings were subjected to oxidation tests for preliminary studies. Stability of the films internal structures was verified by GAXRD and the results with 5° incidence angle are shown in Figure 7. It was verified that at 400 °C, pure Cr thin film was totally transformed into Cr₂O₃ while TiN exhibited just an initial degradation. At 600 °C there was an intense raise in background signal of TiN pure film and more peaks related to TiO₂ were identified, characterizing the total film oxidation.

On the other hand, GAXRD analyses of multilayers submitted to 400 °C showed no Cr₂O₃ formation and less intense peaks for TiO₂ were recorded when compared to pure TiN coating. Such fact revealed that Cr and TiN combination in multilayers systems provided a better oxidation resistance to these materials. The best behavior recorded for multilayers may be attributed mainly to the existence of the sixteen internal interfaces, which play a very important role against diffusion of oxidant agents.

Besides that, once TiN in multilayers tends to grow in the more compact TiN(200) plane, as discussed early in section 3.2, its layers present grains with less empty spaces than pure TiN coating with TiN(111) main peak. Therefore, TiN top layers in multilayers must prevent oxygen diffusion from the surface more efficiently, protecting inner less resistant Cr layers against oxidation.

Graded multilayer M3 tested at 400 °C presented a slight decrease of main peak Cr(110). Given that this sample possesses a top period with TiN/Cr ratio = 4/1 (TiN layer with only 20 nm thick followed by a Cr layer with 80 nm), by a comparative analysis with other films, it is understood that the thinnest TiN top layer was more easily oxidized, favoring the oxygen diffusion to the subsequent Cr layer. Such effect is not seen in M1 sample, which has the same

top TiN layer of 20 nm thickness, probably due to the thinner Cr layer in the top period in comparison to M3 sample.

In this context, it is assumed that greater quantities of the metallic material on the surface period may harm the oxidation resistance and the design of thicker TiN layers on the surface provides better protection to Cr layers. The protective effect of thicker TiN layers on the surface can yet be noticed at 600 °C, since M2 sample with thicker superficial TiN layer

(TiN/Cr = 1/4) still presented a similar GAXRD pattern to as deposited sample whereas other multilayers noticeably manifested an initial distortion of main peak Cr(110).

Aiming to better understand the dynamics of coatings degradation after oxidation tests, cross section and surface micrographs of all oxidized samples were registered. Figure 8a shows sample M1 oxidized at 400°C. Through the image it is possible to note that no holes nor internal defects were formed, with layer sizes and number of TiN/Cr interfaces equivalent to those of as deposited M1 sample. Such behavior was observed for all samples, in other words, none of the films presented architecture modifications at 400°C and the images of all tested multilayers at such temperature were similar to the respective as deposited films (Figure 3). Thus, initial oxidation revealed by GAXRD analyses in such temperature can be exclusively attributed to the films outer layer, not altering original architectures.

Similar results were again observed for samples TM and M2 tested at 600 °C, that is, all of them maintained the architectures presented in Figure 3. However, for hierarchical multilayer M1 and graded multilayer M3, although inner periods of coatings maintained their integrity, it was not possible to identify TiN/Cr interface of the first period, as can be seen in 8b. Noticeably occurred the formation of an irregular layer with bubbles on the surface occurred due to oxide formation, as can be seen at the top of coatings.

According to GAXRD analyses, such layer must be attributed both to TiO₂ and Cr₂O₃ formation, characterizing the degradation of the first multilayer period. In this sense, it is evidenced that architectures with thicker TiN top layer demonstrated an improved oxidation resistance. Therefore, it is evidenced that although M1 coating with hierarchical architecture presents a tendency for mechanical properties improvement, their surface tends to be more easily oxidized or rearranged.

Based on results at 400 and 600 °C, further investigations were performed at 750 °C in order to analyze the multilayers behavior in a higher temperature. GAXRD results of these analyses are shown in Figure 9. It can be observed that none of the films integrally resisted to such temperature, with the formation of TiO₂ and Cr₂O₃ oxides in all multilayers. M3 sample analysis showed more pronounced Cr₂O₃ peaks due to its thicker Cr layers at upper half of the film.

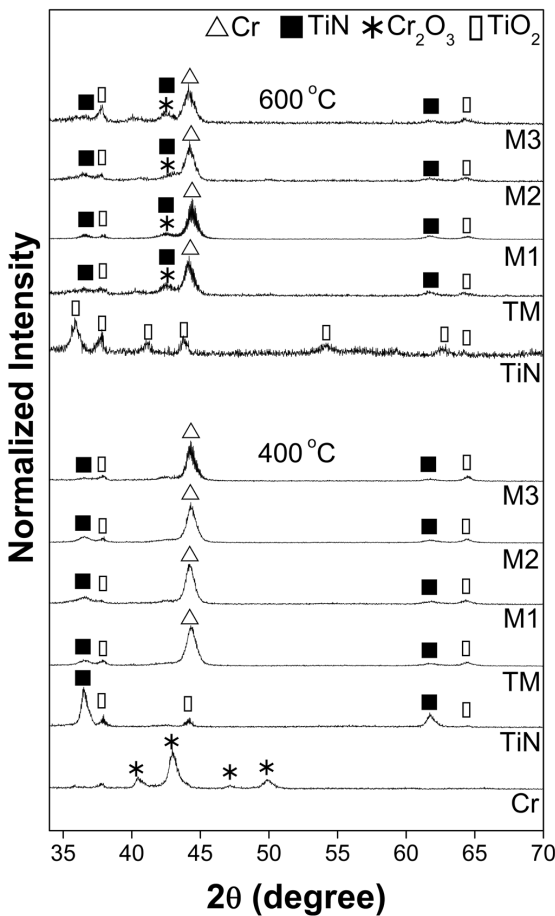


Figure 7. GAXRD patterns of coatings oxidized at 400 °C and 600 °C.

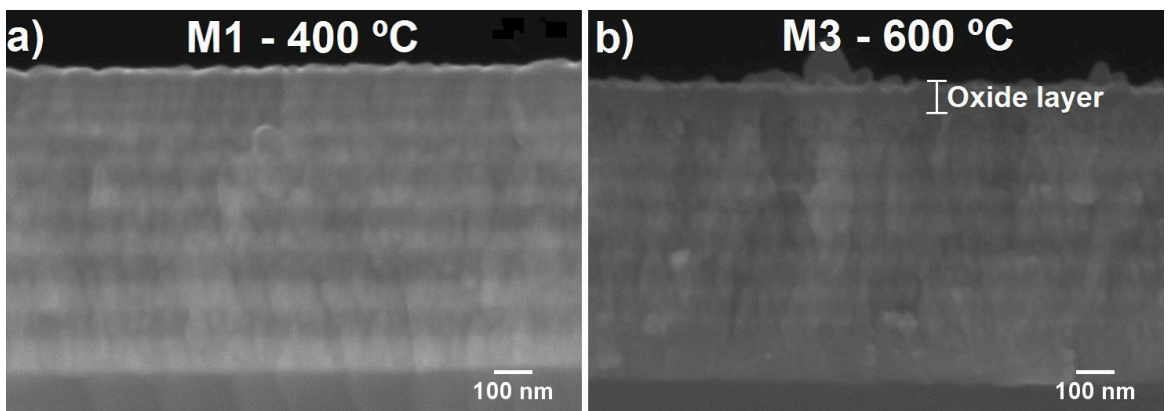


Figure 8. Cross-section SEM images with magnification of 50000x acquired after oxidation tests at (a) 400 °C and (b) 600 °C.

Cross sections of samples oxidized at 750 °C were also evaluated by SEM-FEG, as presented in Figure 10. As evidenced in Figure 10a, all multilayers presented a thicker superficial oxide layer and none of them resisted to oxidation experiments. M1 sample presented in Figure 10b did not maintain original hierarchical structure, with several delamination points between layers, as indicated by the red arrows. In parallel, M2 sample shown in Figure 10c had its

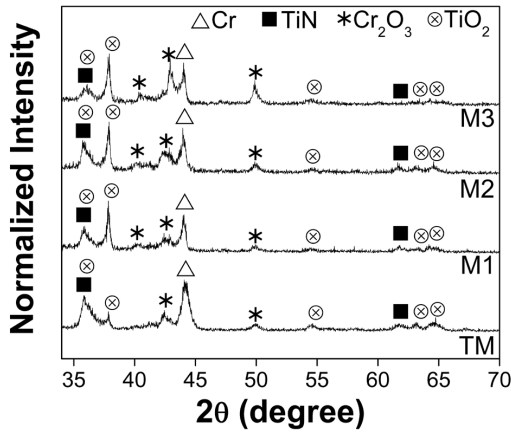


Figure 9. GAXRD patterns of coatings oxidized at 750°C.

internal architecture completely degraded. Considering M2 original structure, in which the TiN top layer is the thickest among samples (80 nm), it is understood that the high and more aggressive temperature of 750 °C overcome TiN(200) layer protective effect. Besides that, since thicker layers are more prone to small defects where oxidation processes may increase significantly, the thicker TiN layer favored oxygen diffusion in the interior of M2 coating, promoting a more intense degradation.

Although TM and M3 samples presented in Figure 10a and Figure 10d, respectively, show the formation of a thicker superficial oxide layer, TiN/Cr internal interfaces were more conserved after oxidation tests at 750°C. Such fact probably is attributed to Cr₂O₃ sub product identified in GAXRD analyses, which has already been reported to block oxygen diffusion and protect multilayer systems¹⁶.

In this context, graded multilayer M3 with more Cr in the first period presented an oxide layer slightly less thick than that registered for iso structured TM sample. However, both samples were decomposed and suffered delamination, as pointed out by the arrows. Once these materials have different thermal expansion coefficients they elongate with different intensities at high temperatures, favoring detachment of TiN/Cr interfaces. Therefore, it is evidenced that TiN/Cr multilayers produced in this work are not suitable for high temperature applications equal or higher than 750 °C.

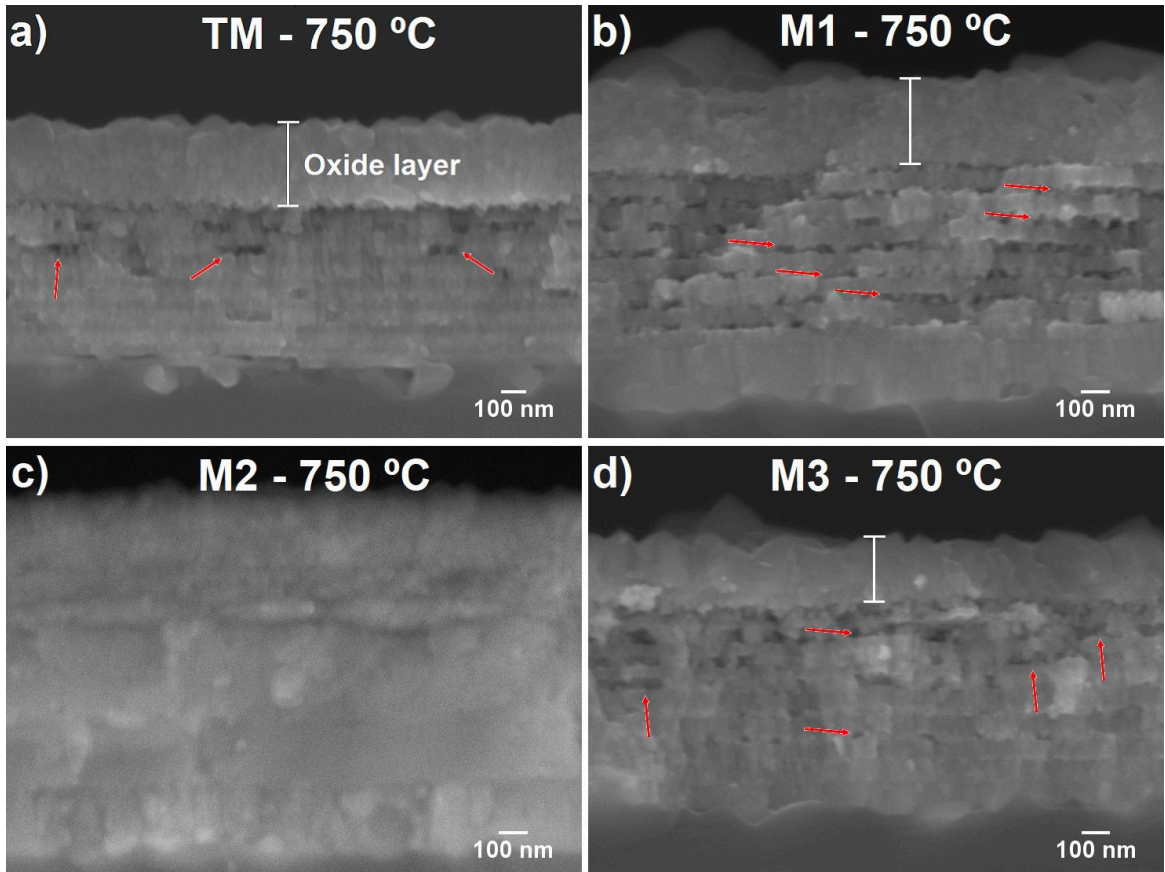


Figure 10. Cross-section SEM images with a magnification of 30000x acquired after oxidation tests at 750 °C.

4. Conclusions

Iso and non-iso TiN/Cr multilayers with different architectures were successfully deposited by magnetron sputtering. Layer sizes influenced the microstructure, presenting columnar-like grains in layers thicker than 50 nm while smaller layers restricted this type of growth. Multilayers presented individual α -Cr and δ -TiN phases connected by incoherent interfaces which prevent diffusion of atoms between neighboring regions in the as deposited coatings. GAXRD analyses showed that TiN superposition to the metallic layers inhibited the common growing in plane TiN(111), though growth increases in plane TiN(200) for layers thicker than 50 nm.

Nanoindentation tests showed hardness values for all multilayers of around 16.2 GPa, evidencing that distribution order of the similar layers did not influence this property. Even so, it was detected a tendency in hierarchical architecture to improve hardness due to Hall-Petch relation. Young's modulus followed the rule of mixtures, indicating total composition of films as the main variable governing it.

TiN/Cr multilayers increased TiN and Cr resistance against oxidation up to 600 °C. Among all tested architectures, samples with thicker TiN top layer presented better oxidation resistance, with emphasis on the graded multilayer M2 with a TiN top layer of 80 nm probably due to a barrier created by the more compact TiN(200) plane. However, TiN/Cr multilayers with total thickness of 800 nm proved to be inefficient for use in atmospheric environments where the temperature is 750 °C or above.

5. Acknowledgements

The authors thank CNPQ, CAPES, FAPESP [grant number 2019/00757-0] and FAPITEC/SE for financial support.

6. References

- Arias DF, Gómez A, Vélez JM, Souza RM, Olaya JJ. A mechanical and tribological study of Cr/CrN multilayer coatings. *Mater Chem Phys.* 2015;160:131-40. <http://dx.doi.org/10.1016/j.matchemphys.2015.04.015>.
- Wang D, Hu M, Jiang D, Fu Y, Wang Q, Yang J, et al. The improved corrosion resistance of sputtered CrN thin films with Cr-ion bombardment layer by layer. *Vacuum.* 2017;143:329-35. <http://dx.doi.org/10.1016/j.vacuum.2017.06.040>.
- Mo J, Wu Z, Yao Y, Zhang Q, Wang Q. Influence of Y-addition and multilayer modulation on microstructure, oxidation resistance and corrosion behavior of Al_{0.67}Ti_{0.33}N coatings. *Surf Coat Tech.* 2018;342:129-36. <http://dx.doi.org/10.1016/j.surfcoat.2018.02.071>.
- Yonekura D, Fujita J, Miki K. Fatigue and wear properties of Ti-6Al-4V alloy with Cr/CrN multilayer coating. *Surf Coat Tech.* 2015;275:232-8. <http://dx.doi.org/10.1016/j.surfcoat.2015.05.014>.
- Renzelli M, Mughal MZ, Sebastiani M, Bemporad E. Design, fabrication and characterization of multilayer Cr-CrN thin coatings with tailored residual stress profiles. *Mater Des.* 2016;112:162-71. <http://dx.doi.org/10.1016/j.matdes.2016.09.058>.
- Adams DP. Reactive multilayers fabricated by vapor deposition: a critical review. *Thin Solid Films.* 2015;576:98-128. <http://dx.doi.org/10.1016/j.tsf.2014.09.042>.
- Raghavan R, Wheeler JM, Esqué-de los Ojos D, Thomas K, Almandoz E, Fuentes GG, et al. A Mechanical behavior of Cu/TiN multilayers at ambient and elevated temperatures: stress-assisted diffusion of Cu. *Mater Sci Eng A.* 2015;620:375-82. <http://dx.doi.org/10.1016/j.msea.2014.10.023>.
- Zhang Y, Xu G, Wang Y, Zhang C, Feng S, Suo J. Mechanical properties study of W/TiN/Ta system multilayers. *J Alloys Compd.* 2017;725:283-90. <http://dx.doi.org/10.1016/j.jallcom.2017.07.115>.
- Lin Y, Zia AW, Zhou Z, Shum PW, Li KY. Development of diamond-like carbon (DLC) coatings with alternate soft and hard multilayer architecture for enhancing wear performance at high contact stress. *Surf Coat Tech.* 2017;320:7-12. <http://dx.doi.org/10.1016/j.surfcoat.2017.03.007>.
- Rivera-tello CD, Broitman E, Flores-ruiz FJ, Jiménez O, Flores M. Mechanical properties and tribological behavior at micro and macro-scale of WC/WCN/W hierarchical multilayer coatings. *Tribol Int.* 2016;101:194-203. <http://dx.doi.org/10.1016/j.triboint.2016.04.017>.
- Song G, Yang X, Xiong G, Lou Z, Chen L. The corrosive behavior of Cr/CrN multilayer coatings with different modulation periods. *Vacuum.* 2013;89:136-41. <http://dx.doi.org/10.1016/j.vacuum.2012.02.046>.
- Liu Y, Shi W, Tian L, Li T, Wang C, Liu F, et al. Influence of modulation period on structure and mechanical properties of WB2/CrN films deposited by direct-current magnetron sputtering. *J Alloys Compd.* 2019;788:729-38. <http://dx.doi.org/10.1016/j.jallcom.2019.02.188>.
- Liu H, Yang F, Tsai Y, Wang X, Li W, Chang C. Effect of modulation structure on the microstructural and mechanical properties of TiAlSiN/CrN thin films prepared by high power impulse magnetron sputtering. *Surf Coat Tech.* 2019;358:577-85. <http://dx.doi.org/10.1016/j.surfcoat.2018.11.069>.
- Nam ND, Kim MJ, Jo DS, Kim JG, Yoon DH. Corrosion protection of Ti/TiN, Cr/TiN, Ti/CrN and Cr/CrN multi-coatings in simulated proton exchange membrane fuel cell environment. *Thin Solid Films.* 2013;545:380-4. <http://dx.doi.org/10.1016/j.tsf.2013.07.056>.
- Ezazi MA, Quazi MM, Zalnezhad E, Sarhan AAD. Enhancing the tribo-mechanical properties of aerospace AL7075-T6 by magnetron-sputtered Ti/TiN, Cr/CrN & TiCr/TiCrN thin film ceramic coatings. *Ceram Int.* 2014;40(10):15603-15. <http://dx.doi.org/10.1016/j.ceramint.2014.07.067>.
- Xiao W, Chen H, Liu X, Tang D, Deng H, Zou S, et al. Thermal shock resistance of TiN-, Cr-, and TiN/Cr-coated zirconium alloy. *J Nucl Mater.* 2019;526:151777. <http://dx.doi.org/10.1016/j.jnucmat.2019.151777>.
- Ye Y, Yao Y, Chen H, Guo S, Li J, Wang L. Structure, mechanical and tribological properties in seawater of multilayer TiSiN/Ni coatings prepared by cathodic arc method. *Appl Surf Sci.* 2019;493:1177-86. <http://dx.doi.org/10.1016/j.apsusc.2019.07.140>.
- Gong Z, Jia X, Ma W, Zhang B, Zhang J. Hierarchical structure graphitic-like/MoS₂ film as superlubricity material. *Appl Surf Sci.* 2017;413:381-6. <http://dx.doi.org/10.1016/j.apsusc.2017.04.057>.
- Yao SH, Su YL, Kao WH, Cheng KW. A wear-resistant coating: oxidized graded multilayer TiN/W coating. *Mater Lett.* 2010;64:99-101. <http://dx.doi.org/10.1016/j.matlet.2009.10.026>.
- Carpio P, Salvador MD, Borrell A, Sánchez E. Thermal behaviour of multilayer and functionally graded YSZ/Gd₂Zr₂O₇ coatings. *Ceram Int.* 2016;43(5):4048-54. <http://dx.doi.org/10.1016/j.ceramint.2016.11.178>.
- Huang C, Chen Y. Design and impact resistant analysis of functionally graded Al₂O₃-ZrO₂ ceramic composite. *Mater Des.* 2016;91:294-305. <http://dx.doi.org/10.1016/j.matdes.2015.11.091>.
- Oliver WC, Pharr GM. An improved technique for determining hardness and elastic modulus. *J Mater Res.* 1992;7(6):1564-83. <http://dx.doi.org/10.1557/jmr.1992.1564>.
- Li L, Guo P, Liu L, Li X, Ke P, Wang A. Structural design of Cr/GLC films for high tribological performance in artificial seawater: Cr/GLC ratio and multilayer structure. *J Mater*

- Sci Technol. 2018;34:1273-80. <http://dx.doi.org/10.1016/j.jmst.2017.12.002>.
24. Nie Y, Dong L, Wu J, Li D. A design of Ti-6Al-4V/ZrB₂ multilayers with good thermal stability to enhance mechanical properties of titanium alloy. *Ceram Int*. 2018;44(5):4704-10. <http://dx.doi.org/10.1016/j.ceramint.2017.12.052>.
 25. Chen S, Luo D, Zhao G. Investigation of the properties of Ti_xCr_{1-x}N coatings prepared by cathodic arc deposition. *Phys Procedia*. 2013;50:163-8. <http://dx.doi.org/10.1016/j.phpro.2013.11.027>.
 26. Aouadi SM, Wong KC, Mitchell KAR, Namavar F, Tobin E, Mihut DM, et al. Characterization of titanium chromium nitride nanocomposite protective coatings. *Appl Surf Sci*. 2004;229:387-94. <http://dx.doi.org/10.1016/j.apsusc.2004.02.019>.
 27. Vishnyakov VM, Bachurin VI, Minnebaev KF, Valizadeh R, Teer DG, Colligon JS, et al. Ion assisted deposition of titanium chromium nitride. *Thin Solid Films*. 2006;497(1-2):189-95. <http://dx.doi.org/10.1016/j.tsf.2005.05.005>.
 28. Postolnyi BO, Beresnev VM, Abadias G, Bondar OV, Rebouta L, Araujo JP, et al. Multilayer design of CrN/MoN protective coatings for enhanced hardness and toughness. *J Alloys Compd*. 2017;725:1188-98. <http://dx.doi.org/10.1016/j.jallcom.2017.07.010>.
 29. Zhang G, Wang T, Chen H. Microstructure, mechanical and tribological properties of TiN/Mo₂N nano-multilayer films deposited by magnetron sputtering. *Surf Coat Tech*. 2015;261:156-60. <http://dx.doi.org/10.1016/j.surfcoat.2014.11.041>.
 30. Rivera-tello CD, Broitman E, Flores-Ruiz FJ, Perez-Alvarez J, Flores-Jiménez M, Jiménez O, et al. Micro and macro-tribology behavior of a hierarchical architecture of a multilayer TaN/Ta hard coating. *Coatings*. 2020;10(263):1-14. <http://dx.doi.org/10.3390/coatings10030263>.
 31. Hall EO. The deformation and ageing of mild steel: III discussion of results. *Proc Phys Soc B*. 1951;64(9):747-53. <http://dx.doi.org/10.1088/0370-1301/64/9/303>.
 32. Petch NJ. The cleavage strength of polycrystals. *Journal of the Iron and Steel Institute*. 1953;174:25-8.